

Low Voltage Low Power Applications Of 3T Gain Cell

Padma Priya. M, Sasikala. P

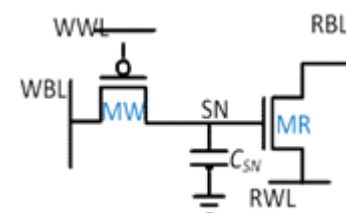
PG Scholar, Dept.of ECE, Gnanamani College of Technology, Namakkal, India.
PG Scholar, Dept.of ECE, Gnanamani College of Technology, Namakkal, India.

Abstract: Logic compatible gain cell (GC)-embedded DRAM (eDRAM) arrays are considered an alternative to SRAM due to their small size, nonratioed operation, low static leakage, and two-port functionality. However, traditional GC-eDRAM implementations require boosted control signals in order to write full voltage levels to the cell to reduce the refresh rate and shorten access times. These boosted levels require either an extra power supply or on-chip charge pumps, as well as nontrivial level shifting and toleration of high voltage levels. In this brief, we present a novel, logic compatible, 3T GC-eDRAM bitcell that operates with a single-supply voltage and provides superior write capability to the conventional GC structures. The proposed circuit is demonstrated with a 2-kb memory macro that was designed and fabricated in a mature 0.18- μm CMOS process, targeted at low-power, energy-efficient applications. The test array is powered with a single supply of 900 mV, showing a 0.8-ms worst case retention time, a 1.3-ns write-access time, and a 2.4-pW/bit retention power. The proposed topology provides a bitcell area reduction of 43%, as compared with a redrawn 6-transistor SRAM in the same technology, and an overall macro area reduction of 67% including peripherals.

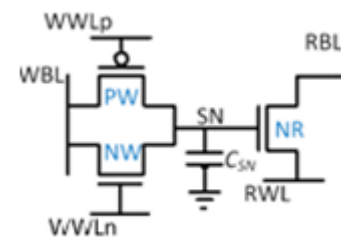
Index Terms: Access speed, data retention time, embedded DRAM, gain cell, low power operation.

1. INTRODUCTION

In recent years, memories have occupied increasingly large portions of the die area of VLSI systems-on-chip (SoCs), in general, and of microprocessors, in particular, as shown in [1]. This is due to the large 6-transistor (6T) SRAM bitcell and its area-consuming peripheral circuitry that are the basis for the vast majority of these. In addition, the standby power of ultralow-power (ULP) systems, such as biomedical implants and wireless sensor networks, is often dominated by embedded memories, which continue to leak during the long retentive standby periods that characterize these systems. The 6T SRAM has been the traditional choice for the implementation of embedded memories due to its high-access speed and refresh-free static data retention. However, the 6T bitcell has several drawbacks in modern systems, including its large transistor count, its impeded functionality under voltage scaling, and the aforementioned static leakage currents from the supply voltage (VDD) to GND. One of the interesting alternative implementations that addresses these limitations, while continuing to provide full CMOS logic compatibility, is gain-cell (GC)-embedded DRAM (eDRAM), such as the circuit shown in Fig. 1(a) [2]–[5]. Most often consisting of 2-transistor (2T) or 3-transistor (3T), GC-eDRAMs provide a reduced silicon footprint, along with inherent two-port functionality, nonratioed circuit operation, and very low static leakage currents from VDD to GND. However, as opposed to static memories, such as SRAM, the data retention of GC-eDRAM depends on dynamically stored charge, and thereby requires periodic, power-hungry refresh operations.



(a) 2T mixed GC.



(b) proposed 3T GC

Fig. 1 Schematic of conventional and proposed GCs.

The data retention time (DRT) of GC-eDRAMs is the time interval from writing a data level into the bitcell to the last moment at which one can still correctly read out the stored information. The DRT is primarily limited by the initial charge stored on the internal bitcell capacitance and the leakage currents that degrade the stored voltage level over time. For traditional 2T and 3T cells, the DRT is significantly affected by the initially degraded voltage level corresponding to data 0 or 1, due to the threshold voltage (V_T) drop across the write transistor [MW in Fig. 1(a)]. In order to address this problem, a boosted write word line (WWL) voltage is usually employed to pass a full swing level to the storage capacitance. However, this requires the generation of a boosted on-chip voltage, which entails substantial overhead [6]. The magnitude of the voltage boost is set not only to overcome the V_T drop, but

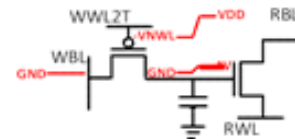
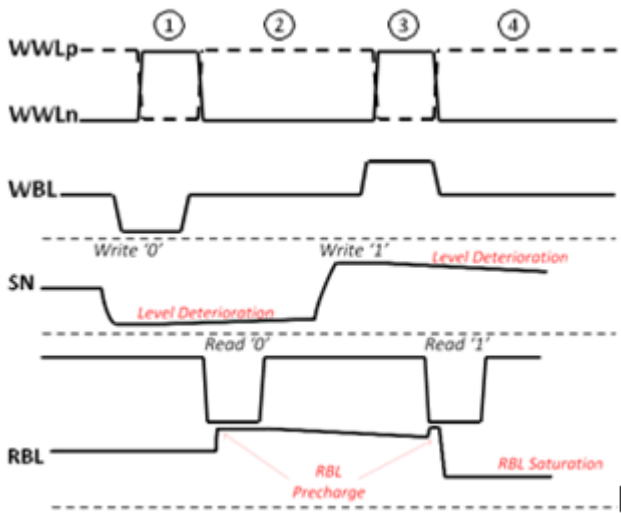
also to achieve short write-access times, which otherwise are typically longer than for 6T SRAM implementations. Furthermore, charge injection (CI) and clock feedthrough (CF) during WWL signal deassertion cause a voltage step at the storage node (SN), resulting in an initially degraded level at the end of a write access [5]. As this undesired coupling even increases with WWL boost magnitude, a clear tradeoff between write speed, power, and DRT is introduced [5]. In addition, the level-shifting and toleration of higher than nominal voltages can be complex, especially when this boosted voltage is a negative underdrive voltage, as required by implementations employing a pMOS MW [2], [4]. The propagation of such a negative voltage can easily lead to voltage drops over device terminals that violate the technology limitations.

lower than a previously reported 6T SRAM at this voltage in the same technology [7].

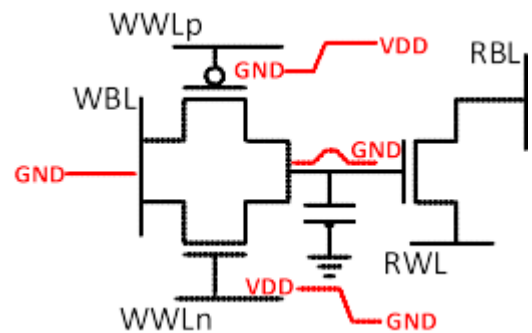
II. PROPOSED 3T GAIN-CELL

A. 3T Gain-Cell Structure

Fig. 1(b) shows the schematic of the proposed single-supply 3T GC. The circuit comprises a write port featuring a complementary TG PMOS Write (PW) and NMOS Write (NW), a read port based on an nMOS device (NR), and a SN composed of the parasitic capacitance (CSN) of the three devices and the stacked metal interconnect. The cell is built exclusively from standard VT transistors and is fully compatible with standard digital CMOS technologies. The gates of PW and NW are connected to the complementary word lines, WWLp and WWLn. A common write bit line (WBL) is used to drive data through the TG during write operations. The full-swing passing capability of the TG enables the propagation of strong levels to the SN without the need for a boosted word line. Read is performed by precharging the read bit line (RBL) and subsequently driving the read word line to GND, thereby conditionally discharging the RBL capacitance if the SN is high (data 1) or blocking the discharge path if the SN is low (data 0). To achieve a reasonable tradeoff between speed, area, power, and reliability, a dynamic sense inverter is used on the readout path (Section III-A). However, other sense amplifiers can be used for improved read performance, such as demonstrated in [3], [8], and [9].



(a)



(b)

Fig.2. Timing diagram of subsequent write and read operations. ① Write 0. ② Read the stored 0. ③ Write 1. ④ Read the stored 1. Plot extracted from Spectre simulations with nominal parameter values.

Contribution: In this brief, we present a new topology for a 3T GC, featuring a complementary transmission gate (TG) in the write port. While the proposed solution is quite straightforward, to the best of our knowledge, it is novel, and its impact is very high, as shown in this brief. The proposed bitcell provides strong initial data levels (both 1 and 0) for enhanced DRT and robust operation, as well as fast write-access times. This dual advantage is achieved without the need for additional voltages or boosted signals, allowing the use of standard peripheral circuitry for simple SoC integration and small silicon area. In order to demonstrate the functionality of the proposed bitcell, a 2-kb memory macro was designed and fabricated in a mature 0.18- μm CMOS node, which is typically used for ULP applications, such as biomedical sensor nodes and implants. The resulting memory macro consumes only 33% of the area of a single-port 6T SRAM macro of the same size in the same technology node. The manufactured 3T GC-eDRAM macro is shown to be fully functional with a single-supply voltage ranging from 600 mV to 1.8 V and a worst case DRT of 0.8 ms at 900 mV, resulting in 4.9 nW/2-kb retention power, which is 17x

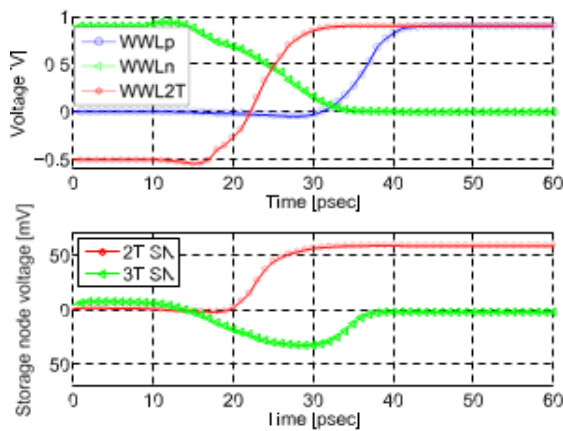


Fig.3. Effects of CI and CF mechanisms. (a) Conventional 2T bitcell. (b) Proposed 3T bitcell. (c) Waveform comparison of the two bitcells during write deassertion

B. 3T Gain-Cell Operation

Fig.2 demonstrates bitcell operation through the application of subsequent write and read operations of both data values with $V_{DD} = 900\text{ mV}$. This supply voltage was chosen as a good median voltage between V_{DD} and V_T , as previously shown to be DRT efficient in GC-eDRAM design [5]. Starting with a charged CSN (1), WBL is driven low and the word lines are asserted ($WWL_p = 0$ and $WWL_n = V_{DD}$). As expected, a strong 0 level is passed to the SN, and this level is retained with the deassertion of the word lines due to the opposing CI and CF effects from the PW and NW transistors. During standby, the level on SN deteriorates due to leakage currents, dominated by the sub- V_T leakage of NW and PW in mature CMOS nodes. Therefore, in order to extend the retention time, WBL is driven to $V_{DD}/2$ during standby and read cycles, thereby significantly reducing the sub- V_T leakage through the TG, for both stored data 0 and 1, compared with the case where WBL is driven to either V_{DD} or GND. The WBL biasing circuitry is described in Section III-A. During readout (2), the 0 level blocks the discharge path through NR, maintaining the precharged voltage on RBL. During the next write operation (3), WBL is driven high, resulting in a strong 1 stored on the SN. The subsequent read operation (4) provides a strong gate overdrive to transistor NR, thereby discharging RBL to read a 1. It should be noted that during this operation (Read 1), bitcells storing 1 and sharing the same column turn on when RBL discharges by more than the V_T of NR, causing it to saturate before it can completely discharge. This phenomenon is common to many GC-eDRAM configurations, as discussed in [5].

C. Comparison With Other Gain-Cell Implementations

A major advantage of the proposed cell over previous 2T and 3T GCs is the self-dampening effect of CI and CF during write, as demonstrated in Fig. 3. For a 2T cell with a pMOS MW [Fig. 3(a)], CI and CF cause a significant positive voltage disturbance

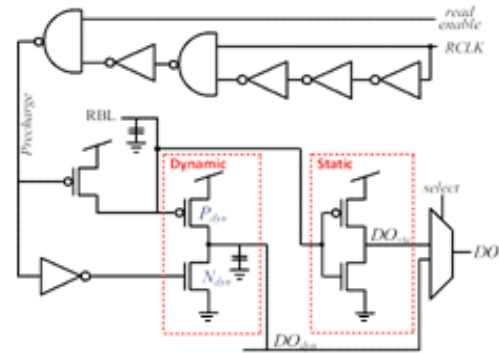


Fig.4. Dynamic readout architecture (c)

on the SN during the rising edge of WWL, resulting in a degraded initial 0 level. However, in the proposed 3T cell [Fig. 3(b)], this problem is avoided due to the opposite transitions of the complementary WWLs (WWL_n and WWL_p), and the opposite polarity of charges injected into CSN from the pMOS and nMOS MWs. This behavior is plotted in Fig. 3(c) for the two configurations with $V_{DD} = 900\text{ mV}$ and an underdrive voltage of -500 mV for the 2T to pass a full 0 level on the falling edge of WWL [5]. Whereas the 2T cell suffers from a degraded level of over 50 mV after WWL deassertion, the CI and CF effects of the complementary devices in the 3T cell essentially negate each other, resulting in a strong 0 V level for this cell. Note that there is still a dip in the 3T SN voltage due to the WWL_n signal transitioning earlier than the WWL_p signal. This could be avoided with more careful timing control. This strong level leads to advantages in both DRT, as well as read-access time, as the initial data levels are stronger.

III. MEMORY MACRO PERIPHERALS

The single-supply voltage required for the operation of the proposed topology simplifies the implementation of a full memory macro is a significant advantage over other GC-eDRAMs using conventional bitcells, which require the use of level shifters to create the desired boosted or negative (dependent on the type of MWs) voltage supply. However, to further improve the array performance, in terms of access time and power consumption, several peripheral techniques were integrated into the designed memory macro. These peripheral circuits and techniques are presented in the following sections.

A. Readout Circuitry

Many previous low-voltage embedded memories, targeted at ULP systems, employ a simple sense inverter in order to provide robust, low-area, and low-power data readout. However, such an inverter suffers from a very slow readout, as it requires the RBL to be discharged (charged for a pMOS read device) past the switching threshold of the inverter, which is hard to deviate away from $V_{DD}/2$. This operation is further impeded by the aforementioned RBL saturation during readout that slows down the discharging (charging) operation, as the RBL voltage decreases (increases). Therefore, the readout path that was integrated into the proposed 3T GC-eDRAM macrocell has two sensing modes: 1) a faster, yet potentially more error-prone, dynamic readout mode and 2) a slightly slower, yet more reliable, static mode. In all measured prototype chips, both

the dynamic (preferred for speed) and static modes were tested successfully. In both sensing modes, Low Threshold device (LVT) pMOS transistors were used in order to allow a faster yet accurate read-access time, due to the aforementioned issues. The supply voltage to the readout circuitry is gated with the read enable signal in order to save substantial static power due to the leaky LVT devices. The schematic of the two alternative readout circuits are shown in Fig. 4. The rising edge of the read clock creates a precharge pulse that charges the parasitic capacitance of RBL and discharges the output capacitance of the dynamic sense inverter (DO_{dyn}) through the discharge transistor, N_{dyn} . Subsequently, RBL is conditionally discharged during the read operation, turning on P_{dyn} to flip the output if a 1 is stored in the selected cell. Therefore, an RBL swing of only one V_T is required to complete a read operation. Transistor sizes for the dynamic sense inverter and pulse generator were chosen according to postlayout simulations under global and local parametric variations.

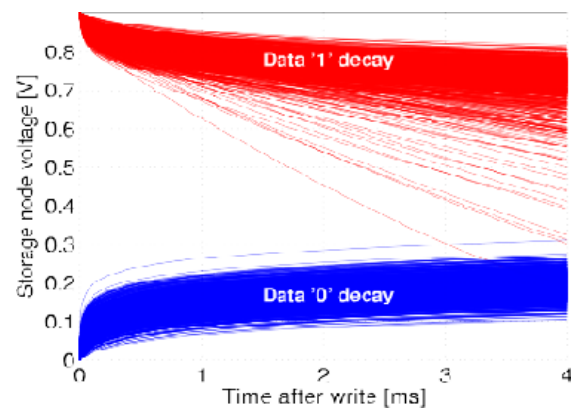
B. Write Circuitry

While the proposed single-supply 3T bitcell provides a significant improvement in both write time and initial SN level over standard GC implementations, the dual-transistor write port adds an additional leakage path to/from the SN. The increased aggregated sub- V_T current causes faster degradation of the stored charge, leading to reduced DRT, as compared with a reference 2T cell. In addition, several previous works have shown that the data dependent, asymmetric DRT (for data 0 and 1) of standard GCs can be manipulated to overall enhance DRTs by biasing the WBL at the best case voltage for the weaker data level during standby and read operations [10]. For the proposed 3T configuration, the worst case DRTs of the 1 and 0 levels are similar, and significant deterioration of the stored levels occurs for both extreme values of WBL bias (V_{DD} and GND). However, a neutral bias of $V_{DD}/2$ can be applied, thereby greatly reducing the sub- V_T current through the TG. Fig. 5 shows the benefit of this measure, displaying the level degradation of stored 1 and 0 data with WBL biases of opposite polarity and $V_{DD}/2$. With a WBL bias of $V_{DD}/2$, the DRT can be extended by $\sim 1000\times$. The write circuitry to implement the median WBL bias during standby and read cycles is shown in Fig. 5(c). A standard inverter chain conditionally drives the data-in level on to the WBL through a TG, controlled by complementary write enable signals Write Enable (WE) and Write Enable Negative (WEN). In parallel, a pair of long-channel I/O devices drive WBL during nonwrite cycles. These devices create a short-circuit path between V_{DD} and GND when WE is low, providing a median potential ($V_{DD}/2$) at WBL. Due to the thick oxides and long channel-lengths of the I/O devices, process variations are significantly reduced, and the static current is extremely low. Based on the chosen transistor sizes, the static power consumption of the proposed WBL driver during nonwrite cycles is only a few femtowatts under a 900-mV supply voltage, which is negligible compared with the refresh power of the array.

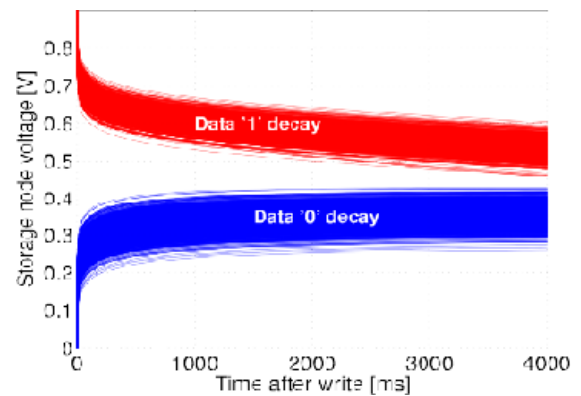
IV. TEST CHIP AND MEASUREMENT RESULTS

A. Implementation and Testing Procedure

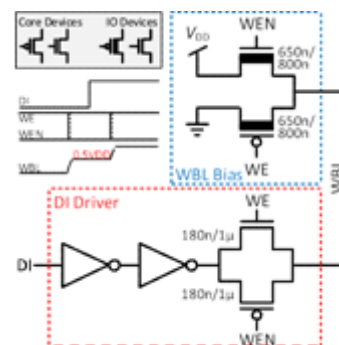
A 64x32 bit (2 kb) memory macro based on the proposed 3T GC was designed in a standard 0.18- μm CMOS process and integrated into a larger test chip with various test structures. All devices were implemented with standard V_T transistors to provide complete logic process compatibility without the need for additional process steps. Minimum-sized MWs were used in order to achieve a small bitcell area, while a slightly wider read transistor was employed in order to improve read-access time. The WWLs were routed with horizontal polysilicon stripes to provide a dense bitcell, while other signals were routed on the first (lowest) three metal layers. Higher interconnect layers (metals 4 and 5) were tightly stacked above the bitcell to increase CSN.



(a)



(b)



(c)

Fig.5.Improved DRT through VDD/2 WBL biasing and the required circuitry. Plots include 1k Monte Carlo samples at 27°C with VDD=0.9V. (a) SN degradation with worst case bias conditions. (b) SN degradation with VDD/2 WBL biasing. (c) Write circuitry for VDD/2 biasing

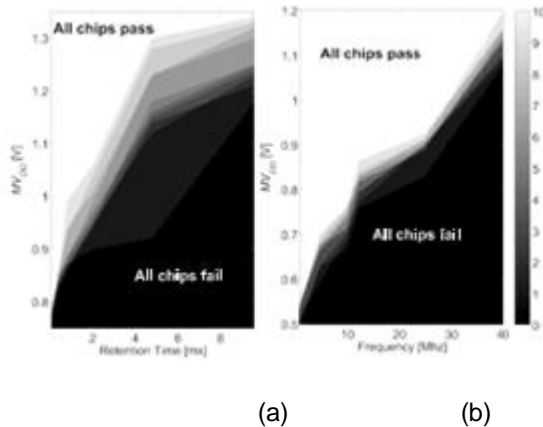


Fig.6. Minimum memory supply voltage Shmooplots for 10m measured chips. (a) Minimum MVDD versus DRT. (b) Minimum MVDD versus frequency.

Fig. 6(a) shows a Shmooplots of MVDD versus the measured DRT for 10 different chips. The grayscale map corresponds to the number of chips that were fully functional for the respective VDD and targeted DRT. The gray levels are a result of global (die-to-die) variations, affecting the DRT of the array for a given MVDD. Even though lowering MVDD results in lower leakage currents from/to the SN, the margin between 1 and 0 levels decreases, resulting in a lower DRT. We note that if this range of DRTs is insufficient previously reported techniques, such as body biasing [11], can be used. The functionality of the memories at different frequencies is shown in Fig. 6(b) for various MVDD voltages, as measured for 10 different chips. The measurement was conducted by writing 1 to all bits of the array and reading them out after the previously measured maximum DRT. The operating frequency was swept for every MVDD to provide the Shmooplots. The array showed full functionality for all frequencies up to 40 MHz with a supply voltage of 1.2 V. Measurements at higher frequencies were impossible due to limitations of the test setup, which was designed for low-frequency ULP applications. The memory frequency is limited by the read-access time, since during readout, RBL needs to discharge in order to flip the sense inverter. This operation strongly depends on the parasitic capacitance of the RBL, as well as the data held in the unselected cells sharing the same column. If any of these cells stores a 1, the RBL discharge saturates at around $VDD - VT$, since at that point the unselected NRs start conducting and counteract the discharging efforts of the selected bit. In addition, due to the fact that readout was performed after the maximum DRT for each VDD, a worst case scenario was measured, since the data in the cells was already deteriorated, making the drive current much lower compared with the case where strong data levels are stored

in the cells. Raising VDD clearly improves the read-access time due to a stronger drive current, which makes the sense inverters switch faster. For a dynamic memory, the relevant metric for static power consumption is retention power, composed of the sum of leakage and refresh power. Retention power was measured for storing an entire array of 0 and 1 under supply voltages ranging from 600 mV to 1.2 V. Leakage power mainly consists of sub-VT currents from the SN to the WBL, which is biased at MVDD/2 during standby periods. The measured retention power was found to be 4.9 nW for MVDD = 900 mV and 1.01 μ W for MVDD = 1.2 V, which is 17x lower than a previously reported 6T SRAM cell [7], operated at 1.2 V in the same technology node (consuming 26 μ W standby power with VDD = 1.8 V). The refresh frequency for every MVDD was selected according to previously measured minimum DRTs.

V. CONCLUSION

This brief proposes a novel 3T GC eDRAM macro cell targeted at ULP systems and providing high storage density. The proposed GC is operated from a single-supply voltage, eliminating the need for boosted voltages, commonly found in prior-art implementations. The proposed cell exhibits faster write-access than conventional GC circuits, while minimizing CI and CF through effects, thereby increasing DRTs and reducing refresh power consumption. The cell area is only 57% of a redrawn 6T SRAM in the same technology, making it a suitable alternative to SRAM for low-power memories. A test-chip containing a 2-kb memory macro based on the proposed 3T GC was fabricated in a mature 0.18- μ m CMOS technology and several chips were tested. Measurement results show full functionality at voltages ranging from 600 mV to 1.8 V with retention power as much as 17x lower than a previously reported 6T SRAM in the same technology node.

REFERENCES

- [1] (2013). International Technology Roadmap for Semiconductors-2013 Edition. [Online]. Available: <http://www.itrs.net>
- [2] D. Somasekharet al., "2 GHz 2 Mb 2T gain cell memory macro with 128 GBytes/sec bandwidth in a 65 nm logic process technology," IEEE J. Solid-State Circuits, vol. 44, no. 1, pp. 174–185, Jan. 2009.
- [3] K. C. Chun, P. Jain, T.-H. Kim, and C. H. Kim, "A 667 MHz logic compatible embedded DRAM featuring an asymmetric 2T gain cell for high speed on-die caches," IEEE J. Solid-State Circuits, vol. 47, no. 2, pp. 547–559, Feb. 2012.
- [4] Y. Lee, M.-T. Chen, J. Park, D. Sylvester, and D. Blaauw, "A 5.42nW/kB retention power logic-compatible embedded DRAM with 2T dual-Vt gain cell for low power sensing applications," in Proc. IEEE A-SSCC, Nov. 2010, pp. 1–4.
- [5] P. Meinerzhagen, A. Teman, R. Giterman, A. Burg, and A. Fish, "Exploration of sub-VT and near-VT 2T gain-cell memories for ultra-low power

- applications under technology scaling,” *J. Low Power Electron. Appl.*, vol. 3, no. 2, pp. 54–72, 2013.
- [6] A. Raychowdhury et al., “PVT-and-aging adaptive wordline boosting for 8T SRAM power reduction,” in *Proc. IEEE ISSCC*, Feb. 2010, pp. 352–353.
- [7] G. M. S. Reddy and P. C. Reddy, “Design and implementation of 8k-bits low power SRAM in 180nm technology,” in *Proc. IMCECS*, vol. 2. 2009, pp. 1–8.
- [8] K. C. Chun, P. Jain, J. H. Lee, and C. H. Kim, “A 3T gain cell embedded DRAM utilizing preferential boosting for high density and low power ondiecaches,” *IEEE J. Solid-State Circuits*, vol. 46, no. 6, pp. 1495–1505, Jun. 2011.
- [9] K. C. Chun, W. Zhang, P. Jain, and C. H. Kim, “A 2T1C embedded DRAM macro with no boosted supplies featuring a 7T SRAM based repair and a cell storage monitor,” *IEEE J. Solid-State Circuits*, vol. 47, no. 10, pp. 2517–2526, Oct. 2012.
- [10] A. Teman, P. Meinerzhagen, R. Giterman, A. Fish, and A. Burg, “Replica technique for adaptive refresh timing of gain-cell-embedded DRAM,” *IEEE Trans. Circuits Syst. II, Exp. Briefs*, vol. 61, no. 4, pp. 259–263, Apr. 2014.
- [11] P. Meinerzhagen, A. Teman, A. Fish, and A. Burg, “Impact of body biasing on the retention time of gain-cell memories,” *J. Eng.*, vol. 1, no. 1, pp. 2051–3305, 2013.
- [12] W. Zhang, K. C. Chun, and C. H. Kim, “A write-back-free 2T1D embedded DRAM with local voltage sensing and a dual-row-access low power mode,” *IEEE Trans. Circuits Syst. I, Reg. Papers*, vol. 60, no. 8, pp. 2030–2038, Aug. 2013.